Volume 23, No 2 | International Journal of Radiation Research, April 2025

Image Quality and Radiation Dose of Portal Venous Imaging by Dual-Source Computed Tomography Single Energy Technology

X. Li, Z. Liang, Y. Duan, W. Liu, Z. Han, R. Wang*

Department Radiology Department, Beijing Shijitan Hospital, Beijing 100038, China

► ***Original article***

***Corresponding author:**
Rengui Wang, M.D.,
E-mail:
wangrenguibj@163.com

Received: October 2023
Final revised: April 2024
Accepted: June 2024

Int. J. Radiat. Res., April 2025; 23(2): 305-309

DOI: 10.61186/ijrr.23.2.305

Keywords: *Computed tomography, radiographic image enhancement, portal vein, radiation dosage, signal-to-noise ratio.*

ABSTRACT

Background*:** The design of this work was to explore the feasibility of optimizing computed tomography (CT) portal vein image quality and radiation dose by virtual single-energy imaging technology. ***Materials and Methods: Nighty-two patients who underwent dual-source CT (DSCT) examination in our hospital from September 2021 and August 2022 were selected as the study objects. They received CT scanning (90/Sn150 kV) and the images of 40 keV to 100 keV and M_0.6 linear fusion were obtained. The signal-to-noise ratio (SNR), contrast-to-noise ratio (CNR), subjective image quality, and radiation dose of different models were calculated. ***Results:*** Statistical significance in the subjective score of image quality was tested among all groups, and the 40 keV group had the highest score. The SD values in 40 keV to 60 keV were elevated, while were declined in 80 keV to 100 keV compared with the M_0.6 fusion image. CNR values in 40 keV to 70 keV groups were significantly higher, and in 90 keV to 100 keV were lower than those in M_0.6 group. SNR in the 40 keV group was significantly better than that in M_0.6 group. The average radiation doses were 6.12 ± 1.30 CTDIvol (mGy) and the radiation dose length product (DLP) was 304.3 ± 87.67 (mGy.cm). ***Conclusion:*** DSCT virtual single energy reconstruction technology could greatly improve image quality, and 40 keV single energy reconstruction had the best image quality.

INTRODUCTION

The hepatic portal vein is mostly made up of the confluence of the superior mesenteric vein and splenic vein behind the pancreatic neck, which are divided into left and right branches at the hepatic hilum, entering the left and right lobes of the liver respectively [1]. Portal venous system thrombotic disease is a common complication in liver cirrhosis cases, with a prevalence in patients with acutely decompensated liver cirrhosis and chronic liver disease [2, 3]. The symptoms of patients with portal vein disorders vary from mild cases with no obvious symptoms or accompanied by abdominal pain to severe cases with prehepatic portal hypertension, aggravated esophageal and gastric varices, and progression of hematemesis, melena, ascites, and even liver failure [4]. When it combines with superior mesenteric vein thrombosis, it may cause intestinal necrosis or even septic shock [5]. Thus, differentiating the severity of portal vein disease is indispensable for the overall treatment, staging, and prognosis of patients with liver disease.

Computed tomography (CT) possesses a momentous role in the diagnosis of multifarious diseases [6, 7]. Dual-source CT (DSCT) has two kinds of independent tube-detector systems, which can simultaneously obtain the data of materials under different X-ray energy [8]. The materials can be identified according to the different X-ray attenuation values of different materials at high and low energies [9]. DSCT, as one of the conventional imaging examinations, showing irreplaceable value in the clinical diagnosis and treatment of vascular related diseases [10, 11]. With the development of dual-energy research and its post-processing technology, virtual monoenergetic imaging (VMI) is becoming increasing important [12]. VMI can be used to image an object by calculating the attenuation value of the X-ray of the object in a virtual single-level state of the data set generated by X-ray scanning of the object at high and low energy levels. After VMI reconstruction, a series of monochromatic images with high contrast and low noise can be obtained, and the lesions can be displayed well [13]. The monoenergetic plus (MEI+) processing technique utilized by Siemens for the second generation of Monoenergetic images overcomes the limitation of the nonlinear noise curve dependence of the first-generation algorithm and improves the image sharpness. Previous investigation reports that the combination of low kiloelectron volt (keV) MEI+ and iodine maps improves the image quality and diagnostic efficacy of pancreatic ductal adenocarcinoma [14]. Therefore, this

report focuses on this technique in detecting portal vein.

In this study, 92 patients in clinical practice were retrospectively selected for DSCT examination, and 40 keV to 100 keV single-energy images of portal veins were obtained. The differences in overall development quality, radiation dose, and image noise were examined, and the optimal CT image scanning and reconstruction scheme was explored to provide a theoretical basis and operational experience for clinical application of MEI+. This investigation may offer an idea on the investigation of CT image scan, and further provided effective imaging strategy for portal vein.

MATERIALS AND METHODS

Participants recruitment

Patients with no contraindications from Beijing Shijitan HospitalHospital between September 2021 and August 2022 were enrolled for liver CT detection. Inclusion criteria were as follows: (1) No previous organic liver disease; (2) no history of abdominal trauma and operation; (3) no liver disease affecting hepatic feeding artery and drainage vein. Exclusion criteria were defined: (1) hyperthyroidism; (2) patients with iodine contrast allergy; (3) non-adult patients under 18 years of age; (4) other diseases affecting blood circulation. 92 cases were eventually intaken in the study, age ranged from 33-80 years old. The average age was 62.12±11.30 years old and the BMI was 23.33±4.09 kg/m^2. 38 females and 54 males constituted the group. This study was granted by the Beijing Shijitan HospitalHospital ethics committee (approval number: 2020015, 7 April 2020).

Scanning equipment and plans

The scanning equipment was the third generation of DSCT (SOMATOM Force, Siemens Healthcare, Forchheim, Germany). Twenty to thirty minutes before the examination, 500 to 1000 ml of clear water was administered and used as a negative control. At the same time, the case should be trained in breathing, and the abdominal belt should be pressurized when necessary to control the artifacts caused by breathing movement to the greatest extent.

During the routine plain scan, the supine position was applied, ranging from the septum to liver. The condition of scanning was 90 kV (A ball) and Sn150 kV (B ball), and 224 mAs and 140 mAs for tube current. The speed was 0.5 s, collimation was set to 3 × 128 × 0.6 mm and the pitch was 1.0. The contrast agent was heated to 37°C. Double-barreled high-pressure syringe (Medrad, Bayer, Leverkusen, Germany) was selected to inject 80-100 ml of iomeprol contrast medium (350 mg/ml, Bracco, Italy) through the left elbow vein at a rate of 5 ml/s. After injection, 20 ml of normal saline (0.9%) was injected to ensure adequate application of the contrast agent, and the inject rate was same to iomeprol contrast medium. The uppermost abdominal aorta was scanned using the bolus tracking technique, and the threshold was set to 150 hounsfied unit (HU). Dual-energy scanning was triggered in the arterial phase, and then in the portal venous phase after 30 seconds.

Post-scan processing

The scan data is achieved via a Syngovia post-processing workstation (Siemens Healthcare, Erlangen, Germany). First, the linear fusion images with a coefficient of 0.6 were automatically generated. And then the MEI+ algorithm was used to reconstruct the virtual single-energy images of the portal vein at 40-100 keV with an interval of 10 keV and eight different groups of images with 1 mm thicknesses were obtained.

Image quality evaluation

A double-blind assessment of image quality was performed by two radiologists experienced in coronary CT diagnosis. All images were displayed under the optimal window width and window level. The stent structure was displayed using a 5-point scale. 5 points: the shape of portal vein is clear, and there is no obvious image noise, showing 4 branches; 4 points: the shape and details of portal vein are relatively clear, and the image quality is good, showing 3 branches; 3 points: the image quality is medium, there is image noise, and secondary branches can be seen; 2 points: the picture quality is weak, the first-order branch can be seen, and the image noise is obvious; 1 point: has awful image quality, and only the portal vein trunk is displayed [15].

A region of interest (ROI) area of 30 mm^2 was delineated. The CT attenuation values measured in Hounsfield units (HU) of the horizontal main portal vein trunk at the porta hepatis were interpreted as the signal intensity. The objective image noise was the standard deviation (SD) of liver parenchyma. The final value was taken by calculating the average of three times of measurement. The contrast-to-noise ratio (CNR) and signal-to-noise ratio (SNR) of portal vein trunk were computed: CNR = (mean signal intensity of portal vein –mean signal intensity noise)/ image noise, SNR = mean signal intensity y of portal vein /image noise.

Radiation dosage

The radiation dose-length product (DLP), volume CT dose index (CDTIvol), and scan length (cm) were recorded in detail for each participant. Then, according to the average coefficient published by the European Commission in 2004, the effective dose (ED) was computed by the following formula:

ED = 0.0015*DLP [16].

Statistical analysis

Data processing and calculation were performed on statistical package for the Social Sciences (SPSS) 21.0 software package (IBM SPSS; IBM Co, Armonk, NY, USA). The mean value and SD were calculated for measurement data, which were compared using t-test method. $P < 0.05$ indicated that the difference was statistically significant.

RESULTS

Comparison of subjective image quality

The image quality evaluated by two physicians were demonstrated in figure 1. The image quality from the 40 keV groups to 100 keV was gradually declined. The average image quality grade of 40 keV was 4.86±0.15, of 50 keV was 4.53±0.33, of 60 keV was 4.30±0.29, and of 70 keV was 3.99±0.38. The score of M_0.6 group was 3.72±0.50. The quality scores of the 40 keV group to 70 keV group were elevated compared with the M_0.6 group (P<0.001, figure 1). The quality of 80 keV to 100 keV declined, which was statistically different from the M_0.6 group (P<0.01, figure 1).

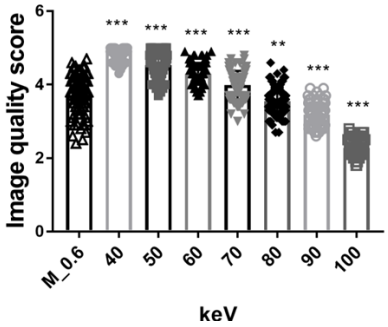

Figure 1. The image quality score was declined with the increase of keV values. **P < 0.01, ***P < 0.001. Error bars mean standard deviation (SD).

An objective analysis of image quality

The attenuation values of portal vein, background image noise, CNR, and SNR were plotted in figure 2 and their mean data summarized in table 1. All these parameters reflected the objective image quality. As shown in Figure 2A, the signal gradually decreased with the increase of keV values. The CT values of 40 keV to 60 keV were elevated compared to the M_0.6 group, while the signal data of 80 keV to 100 keV were decreased (P<0.001, figure 2A). The CT value of M_0.6 group was 205.4±30.91 HU, the highest value was 581.4±107.5 HU in the 40 keV group, and the lowest value was 113.8 ± 13.45 HU in the 100 keV group (table 1). The SD values were increased in the 40 keV to 60 keV groups, which was shown in figure 2B (P<0.001).

The CNR of 40 keV to 60 keV Mono+reconstructed images was higher than that of M_0.6 image (P<0.001, figure 2C). The CNR value increased continuously with the decrease of keV, and it reached its peak at 40 keV, which was 6.87±2.86 (table 1). The SNR values elevated in the 40 keV to 60 keV groups, while they declined in the 90 keV to 100 keV groups (figure 2D, P<0.001). The SNR value in the M_0.6 fusion image was 11.83±2.60, and in the 40 keV image was 13.78±3.08 (table 1).

Table 1. Information of image quality of portal vein.

keV	M_6	40	50	60	70	80	90	100
Portal vein (HU)	205.4 ± 30.91	581.4 ± 107.5	419.5 ± 72.42	289.9 ± 56.18	212.3 ± 37.56	152.2 ± 24.82	142.6 ± 20.20	113.8 ± 13.45
SD of liver parenchyma	17.62 ± 3.61	45.61 ± 9.68	32.40 ± 7.49	21.17 ± 7.84	18.11 ± 3.44	16.15 ± 3.56	15.93 ± 3.24	16.47 ± 34.58
CNR	4.16 ± 1.99	6.87 ± 2.86	5.76 ± 3.40	5.31 ± 2.60	4.29 ± 1.98	3.66 ± 2.06	2.59 ± 1.08	1.78 ± 1.10
SNR	11.83 ± 2.60	13.78 ± 3.08	12.86 ± 3.42	12.19 ± 3.77	11.54 ± 3.04	10.10 ± 3.37	9.02 ± 2.82	7.52 ± 2.60

Note: HU: hounsfied unit, SD: standard deviation, CNR: contrast-to-noise ratio, SNR: signal-to-noise ratio. The values were presented as mean ± standard deviation (SD).

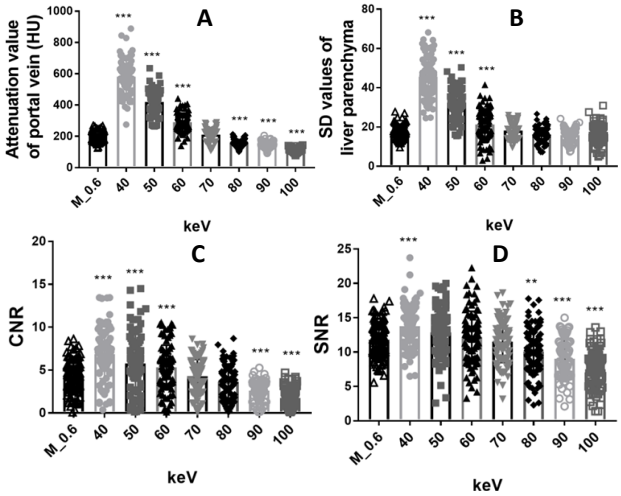

Figure 2. The objective image quality of M_0.6 model and different keV models. **(A)** The comparison on attenuation values between M_0.6 group and other series groups of different keV values. **(B)** The SD values of liver parenchyma. **(C)** The discrepancy of CNR. **(D)** The values of CNR. **P < 0.01, ***P < 0.001. Error bars mean standard deviation (SD).

Radiation dose

The dose received by the patient is mainly represented by CTDIvol and DLP. The CTDIvol was 6.12 ± 1.30 mGy and the DLP was 304.3 ± 87.67 mGy.cm, respectively. The ED value was 4.53 ± 1.24 mSV.

DISCUSSION

The portal vein is anatomically made up of the confluence of the superior mesenteric vein and the splenic vein [17]. It receives blood from the gastrointestinal tract and the spleen and serves as a bridge between the gastrointestinal tract and the liver [18]. The pathological changes in the portal vein system have a great impact on the human body. Due

to the particularity of anatomy and function, the portal vein system is the spreading path of infection and a variety of tumors [19, 20]. At the same time, the portal vein can also be affected by pathological changes in the liver. Portal hypertension can lead to esophagogastric varices or even rupture, resulting in severe complications such as massive gastrointestinal bleeding and hepatic encephalopathy [21].

Spectral CT is obtained by setting high-energy and low-energy X-rays, which can distinguish different kinds of tissues in the body according to attenuation characteristics and produce mono-energy X-ray images [22]. Dual-energy CT can calculate monoenergetic images at any X-ray energy level by using the principle of material separation, so as to realize monoenergetic imaging [23]. A monoenergetic spectral image is the attenuation image obtained after an X-ray at a certain energy level passes through the material [24]. For the monoenergetic spectral image at a certain energy level, the attenuation coefficient of the material depends on its density, which ensures the constant attenuation coefficient of the same material, can avoid the volume effect and hardening effect, and select the best energy value of the output image [25]. In this paper, the value of MEI+ technique in improving image quality and reducing radiation dose was evaluated. The 40 keV groups had the highest CNR and SNR values in the four groups of images, followed by the corresponding values of the 40 keV group. The subjective image quality score of 40 keV group was the highest. The above results indicated that the low VMI+ technique of dual-energy scanning can significantly improve subjective and objective image quality. Consistently, a previous study has presented that DSCT values on VMI at 90 keV had high sensitivity and specificity in differentiating small intrahepatic mass-forming cholangiocarcinoma (IMCC) from small liver abscess (LA) [26].

VMI+ technology is used to reconstruct CT images of tumors or cardiothoracic vascular diseases, including coronary plaque, coronary stent, papillary thyroid carcinoma, and pulmonary embolism [27, 28]. The CNR value and image quality were improved in detecting pancreatic cancer [29]. Martin *et al*. apply the dual-energy CT on patients with portal vein thrombosis and report that the CNR was the highest in 40 keV of other reconstruction images [30]. We estimated the image quality of portal vein images reconstructed by MEI+ algorithm under different energy levels in this study. Different from the previous study, we reconstructed the images every ten keV from 40 keV to 100 keV. In the current study, subjective image evaluation also showed that the 40 keV image was significantly superior to M_0.6 reconstructed image in the portal vein, and was the highest among all groups. The SNR and CNR are crucial items in estimating the objective image quality [31, 32]. Our results showed that the CT values of portal vein in 40 keV MEI+ reconstructed images and their differences were significantly higher in all groups, and CNR and SNR were elevated compared with those reconstructed by linear fusion M_0.6, respectively. Besides, the radiation dose of this detection method was displayed in this research. The average of ED value was 4.53±1.25 mSV.

The present results determined that the MEI+ low-keV image could improve the image quality of portal vein. The optimal energy value of the virtual single energy reconstruction image in the portal vein phase of the DSCT scan was 40 keV, and 70 keV was the closest to the fusion reconstruction image. The prospective study of using this technique is worth further discussion.

ACKNOWLEDGMENT

Not Applicable.

***Declarations of interest*:** No conflict of interest has been declared by the authors.

***Funding*:** This research did not receive any specific grant from funding agencies in the public, commercial, or not-for-profit sectors.

***Ethical consideration*:** This investigation was granted by the Beijing Shijitan Hospital ethics committee (approval number: 2020015, 7 April 2020).

***Author contribution*:** X. L. and Z.Y. L designed experiments, analyzed data and contributed to writing. Y.L. D, W. L and Z.B. H identified and selected patient groups and collected data. R.G. W contributed to writing and manuscript review. All authors read and approved the final manuscript.

REFERENCES

1. Zane KE, Makary MS (2021) Locoregional therapies for hepatocellular carcinoma with portal vein tumor thrombosis. *Cancers, **13**(21): 5430.*
2. Senzolo M, Garcia-Tsao G, Garcia-Pagan JC (2021) Current knowledge and management of portal vein thrombosis in cirrhosis. *J Hepatol, **75***(2): 442-53.
3. Cruz-Ramon V, Chinchilla-Lopez P, Ramirez-Perez O, Aguilar-Olivos NE, Alva-Lopez LF, Fajardo-Ordonez E, *et al.* (2018) Thrombosis of the portal venous system in cirrhotic vs. non-cirrhotic patients. *Ann Hepatol, **17***(3): 476-81.
4. Galante A and De Gottardi A (2021) Portal vein thrombosis: an overview of current treatment options. *Acta Gastroenterol Belg, **84*** (2): 327-32.
5. Zaw ST, Zaw T, El-Far A (2022) Acute mesenteric ischemia secondary to superior mesenteric vein thrombosis. *Cureus, **14**(10): e30819.*
6. Sun B and Wang Z (2024) The application value of computed tomography perfusion imaging in diagnosing early cerebral infarction. *International Journal of Radiation Research, **22***(1)*: 139-43.*
7. Zhao P, Xu Y, Xie C, Zhan M, Qian Y, Gao Z (2024) Assessment of the effectiveness of neoadjuvant chemotherapy for rectal cancer by MRI and PETCT: a meta-analysis. *International Journal of Radiation Research, **22**(1): 85-90.*
8. Baliyan V, Kordbacheh H, Serrao J, Sahani DV, Kambadakone AR (2018) Dual-source dual-energy ct portal venous phase abdominal ct scans in large body habitus patients: preliminary observations on image quality and material decomposition. *J Comput Assist Tomogr, **42**(6): 932-6.*

9. Lu Z, Wu S, Yan C, Chen J, Li Y (2021) Clinical value of energy spectrum curves of dual-energy computer tomography may help to predict pathological grading of gastric adenocarcinoma. *Translational cancer research,* ***10****(1): 1-9.*
10. Chen Q and Zhang C (2023) Dual-source CT imaging in evaluating cardiovascular function after coronary artery bypass grafting. *International Journal of Radiation Research,* ***21****(4): 837-40.*
11. Wang T, Han Y, Lin L, Yu C, Lv R, Han L (2022) Image quality enhancement of CT hepatic portal venography using dual energy blending with computer determined parameters. *J Xray Sci Technol,* ***30****(2): 307-17.*
12. Ren H, Zhen Y, Gong Z, Wang C, Chang Z, Zheng J (2021) Assessment of virtual monoenergetic images in run-off computed tomography angiography: A comparison study to conventional images from spectral detector computed tomography. *Journal of Computer assisted Tomography,* ***45****(2): 232-7.*
13. Li J, Zhao S, Ling Z, Li D, Jia G, Zhao C, Lin X, Dai Y, Jiang H, Wang S (2022) Dual-energy computed tomography imaging in early-stage hepatocellular carcinoma: A preliminary study. *Contrast Media & Molecular Imaging,* ***2022***: *2146343.*
14. Liang H, Zhou Y, Zheng Q, Yan G, Liao H, Du S, Zhang X, Lv F, Zhang Z, Li YM (2022) Dual-energy CT with virtual monoenergetic images and iodine maps improves tumor conspicuity in patients with pancreatic ductal adenocarcinoma. *Insights into Imaging,* ***13****(1): 153.*
15. De Cecco CN, Buffa V, Fedeli S, Luzietti M, Vallone A, Ruopoli R, *et al*. (2010) Dual energy CT (DECT) of the liver: conventional versus virtual unenhanced images. *European Radiology,* ***20****(12): 2870-5.*
16. Liu S, Sheng H, Shi H, Li W, Fan J, He J, Sun H (2018) Computed tomography portography of patients with cirrhosis with normal body mass index: Comparison between low-tube-voltage CT with low contrast agent dose and conventional CT. *Medicine,* ***97****(48): e13141.*
17. Çoruh AG, Uzun Ç, Bozca E, Bozca B, Demir İ B, Atasever HG, *et al*. (2020) Is it possible to predict the side of hepatic metastases according to the primary location of colorectal cancer? *Polish Journal of Radiology,* ***85***: *e595-e9.*
18. Miñano C and Garcia-Tsao G (2010) Clinical pharmacology of portal hypertension. *Gastroenterology clinics of North America,* ***39****(3): 681-95.*
19. Kurimoto A, Yamanaka J, Hai S, Kondo Y, Sueoka H, Ohashi K, *et al.* (2016) Parenchyma-preserving hepatectomy based on portal ramification and perfusion of the right anterior section: preserving the ventral or dorsal area. *Journal of Hepato-Biliary-Pancreatic Sciences,* ***23****(3): 158-66.*
20. Wang L, Wu M, Zhu C, Li R, Bao S, Yang S, Dong J (2022) Ensemble learning based on efficient features combination can predict the outcome of recurrence-free survival in patients with hepatocellular carcinoma within three years after surgery. *Frontiers in Oncology,* ***12***: *1019009.*
21. Wei W, Pu YS, Wang XK, Jiang A, Zhou R, Li Y, Zhang QJ, Wei YJ, Chen B, Li ZF (2017) Wall shear stress in portal vein of cirrhotic patients with portal hypertension. *World Journal of Gastroenterology,* ***23****(18):3279-86.*
22. Han R, Sun K, Lu B, Zhao R, Li K, Yang X (2017) Diagnostic accuracy of coronary CT angiography combined with dual-energy myocardial perfusion imaging for detection of myocardial infarction. *Experimental and Therapeutic Medicine,* ***14****(1): 207-13.*
23. Lai LY, Jiang Y, Shu J (2023) The application of dual-layer spectral detector ct in abdominal vascular imaging. *Current Medical Imaging*, ***19****(14):1609-1615.*
24. Kim C, Lee KY, Shin C, Kang EY, Oh YW, Ha M, Ko CS, Cha J (2018) Comparison of filtered back projection, hybrid iterative reconstruction, model-based iterative reconstruction, and virtual monoenergetic reconstruction images at both low- and standard-dose settings in measurement of emphysema volume and airway wall thickness: A CT phantom study. *Korean journal of radiology,* ***19****(4): 809-17.*
25. Cong W, Xi Y, De Man B, Wang G (2021) Monochromatic image reconstruction via machine learning. *Machine Learning: Science and Technology,* ***2****(2): 025032.*
26. Kim JE, Kim HO, Bae K, Cho JM, Choi HC, Choi DS (2017) Differentiation of small intrahepatic mass-forming cholangiocarcinoma from small liver abscess by dual source dual-energy CT quantitative parameters. *Eur J Radiol,* ***92***: *145-52*.
27. Zeng Y, Geng D, Zhang J (2021) Noise-optimized virtual monoenergetic imaging technology of the third-generation dual-source computed tomography and its clinical applications. *Quantitative Imaging in Medicine and Surgery,* ***11****(11): 4627-43.*
28. Zhou J, Zhou Y, Hu H, Shen MP, Ge YQ, Tao XW, Xu XQ, Su GY, Wu FY (2021) Feasibility study of using virtual non-contrast images derived from dual-energy CT to replace true non-contrast images in patients diagnosed with papillary thyroid carcinoma. *Journal of X-ray Science and Technology,* ***29****(4): 711-20.*
29. Ohira S, Koike Y, Akino Y, Kanayama N, Wada K, Ueda Y, *et al.* (2021) Improvement of image quality for pancreatic cancer using deep learning-generated virtual monochromatic images: Comparison with single-energy computed tomography. *Physica Medica,,* ***85***: *8-14.*
30. Martin SS, Kolaneci J, Czwikla R, Booz C, Gruenewald LD, Albrecht MH, *et al.* (2022) Dual-energy CT for the detection of portal vein thrombosis: improved diagnostic performance using virtual monoenergetic reconstructions. *Diagnostics (Basel, Switzerland),* ***12*** *(7): 025032.*
31. Pinho DF, Kulkarni NM, Krishnaraj A, Kalva SP, Sahani DV (2013) Initial experience with single-source dual-energy CT abdominal angiography and comparison with single-energy CT angiography: image quality, enhancement, diagnosis and radiation dose. *European Radiology,* ***23****(2): 351-9.*
32. Saba L, di Martino M, Siotto P, Anzidei M, Argiolas GM, Porcu M, Suri JS, Wintermark M (2018) Radiation dose and image quality of computed tomography of the supra-aortic arteries: A comparison between single-source and dual-source CT Scanners. *Journal of Neuroradiology,* ***45****(2): 136-41.*